Energy 43 (2012) 427–437

Contents lists available at SciVerse ScienceDirect

Energy

journal homepage: www.elsevier.com/locate/energy

Probabilistic energy and operation management of a microgrid containing wind/photovoltaic/fuel cell generation and energy storage devices based on point estimate method and self-adaptive gravitational search algorithm

Taher Niknam [a,*], Faranak Golestaneh [a], Ahmadreza Malekpour [b,c]

[a] Department of Electrical and Electronic Engineering, Shiraz University of Technology, Iran
[b] Young Researchers Club, Zarghan Branch, Islamic Azad University, Zarghan, Iran
[c] Department of Electrical and Computer Engineering, Kansas State University, Manhattan, KS 66506, USA

ARTICLE INFO

Article history:
Received 15 December 2011
Received in revised form
5 February 2012
Accepted 27 March 2012
Available online 23 May 2012

Keywords:
Energy and operation management
microgrid (MG)
Point estimate method
Self-adaptive gravitational search algorithm (SGSA)
Uncertainty

ABSTRACT

Recently, due to technology improvements, governmental incentives for the use of green energies and rising concerns about high cost of energy from fossil fuels, renewable energy sources (RESs) appears to be a promising approach for producing local, clean, and inexhaustible energy. This motivates the implementation of microgrids (MGs) introduced as a cluster of electrical and/or thermal loads and different RESs. Due to different uncertainties linked to electricity supply in renewable microgrids, probabilistic energy management techniques are going to be necessary to analyze the system. This paper proposes a probabilistic approach for the energy and operation management (EOM) of renewable MGs under uncertain environment. The proposed framework consists of $2m$ point estimate method for covering the existing uncertainties in the MGs and a self-adaptive optimization algorithm based on the gravitational search algorithm (GSA) to determine the optimal energy management of MGs. This paper considers uncertainties in load demand, market prices and the available electrical power of wind farms and photovoltaic systems. In this study, a self-adaptive mutation technique is offered to enhance the convergence characteristics of the original GSA and avoid being entrapped into local optima. The Weibull and normal distributions are employed to model the input random variables. Moreover, the Gram–Charlier expansion is used to find an accurate distribution of the total energy and operational cost of MGs for the next day-ahead. The effectiveness of the proposed method is validated on a typical grid-connected MG including energy storage and different power generating units.

1. Introduction

Recently, development in renewable energy technologies and rising concerns about high cost of energy from fossil fuels and global warming have increased the utilization of distributed energy resource (DER) units [1,2]. Penetration of DER units provides utility owners and customers various benefits such as: lower energy cost, higher service reliability and power quality [3]. The DER units are small energy sources located near local loads and categorized to distributed generation (DG) and distributed storage (DS) units [4]. The DG units include wide range of technologies such as fuel cells, micro turbines (MTs), diesel engines, photovoltaic (PV) systems and small wind turbines (WTs). Likewise, DS units are composed of different types of batteries, energy capacitors, flywheels and controllable loads [5].

The DER units can operate in both grid-connected and autonomous mode. This brings about the concept of microgrid (MG). An MG is defined as a cluster of electrical and/or thermal loads and DER units serviced by a distribution system and expected to remain operational after separation from the system. The energy storage units are used along with the DG ones to make the operation of MGs more reliable and economical [6,7].

Several studies have focused on optimizing the energy and operation management (EOM) of MGs. Chen et al. [5] presented a smart energy management system based on the matrix real-coded genetic algorithm to optimize the operation of MG. A power

Abbreviations: MG, Microgrid; SGSA, self-adaptive gravitational search algorithm; GSA, gravitational search algorithm; DER, distributed energy resource; DG, distributed generation; DS, distributed storage; WT, wind turbine; MT, micro turbine; PV, photovoltaic; EOM, energy and operation management; MGCC, microgrid central controller; PAFC, phosphoric acid fuel cell; NiMH-Battery, nickel-metal-hydride battery; PEM, point estimate method; PDF, probability density function; CDF, cumulative density function; IRV, input random variable; OFE, objective function evaluation; STD, standard deviation.

* Corresponding author.
E-mail address: taher_nik@yahoo.com (T. Niknam).

0360-5442/$ – see front matter © 2012 Elsevier Ltd. All rights reserved.
doi:10.1016/j.energy.2012.03.064

Nomenclature

t, k time interval and iteration index, respectively
n total number of optimization variables
NT total number of hours
N_g, N_s total number of generation and storage units, respectively
N_D total number of load levels
$\tilde{f}(\mathbf{X})$ expected cost
u_i^t status of unit i at hour t
p_{Gi}^t, p_{sj}^t active power output of the ith generator and the jth storage device at time t, respectively
p_{Grid}^t active power bought/sold from/to the utility at time t
B_{Gi}^t,B_{sj}^i bid of the ith DG source and the jth storage device at hour t, respectively
B_{Grid}^t bid of utility at hour t
S_{Gi}, S_{sj} start-up/shut-down costs for the ith DG unit and the jth storage device, respectively
p_{L_D} the amount of the Dth load level
$p_{G,\min}^t$,$p_{G,\max}^t$ minimum and maximum active power production of the ith DG at hour t, respectively
$p_{s,\min}^t$,$p_{s,\max}^t$ minimum and maximum active power production of the jth storage at hour t, respectively
$p_{grid,\min}^t$,$p_{grid,\max}^t$ minimum and maximum active power production of the utility at hour t, respectively
W_{ess}^t, W_{ess}^{t-1} battery energy storage at time t and $t-1$, respectively.
P_{Charge} ($P_{discharge}$) permitted rate of charge (discharge) through a definite period of time Δt
η_{charge} ($\eta_{discharge}$) charge (discharge) efficiency of the battery
$W_{ess,\min}$ ($W_{ess,\max}$) lower and upper bounds on battery energy storage, respectively
$P_{charge,\max}$ ($P_{discharge,\max}$) maximum rate of charge (discharge) during definite period of time Δt
Res^t the scheduled spinning reserve at time t
z_l value of the lth input random variable of the $2m$ point estimate method
$z_{l,po}$ poth standard location of z_l.
$\omega_{l,po}$ poth weighting factor $z_{l,po}$
μ_S, σ_S mean and the standard deviation of the S, respectively
N, Prob($z_{l,j}$) number of observations of z_l and the probability of each observation $z_{l,j}$, respectively
m number of the input random variables of $2m$ point estimate method
$Iter_{max}$ maximum number of iterations
r random number between 0 and 1.
$Iter$ current iteration.
R_{je}^k Euclidean distance between two particles j and e.
ε small constant.
N_{swrm} total number of the bees in the swarm
M_j^k, M_e^k gravitational mass related to particles j and e.
$V_{new,j}^{k,t}$,$V_{old,j}^{k,t}$ new and old velocity of the jth particle, respectively.
$X_{new,j}^{k,t}$,$X_{old,j}^{k,t}$ new and old position of the jth particle, respectively.
G^k gravitational constant at the kth iteration.
$Fit(\mathbf{X}_j^k)$ fitness value of the jth particle.
$Mean^{k,t}$ mean value of the swarm at time t.
$Gl^{k,t}$ best solution found by the swarm up to now.

forecasting module, an energy storage system management module and an optimization module were utilized during the optimization process. Sortomme and El-Sharkawi [8] modeled the load demand and generation of two MGs, including wind farms using optimal power flow and particle swarm optimization (PSO) algorithm. They have shown how selling stored energy at high prices and also performing load peak shaving can reduce the total operational costs. An optimization scheme has been proposed in Ref. [9] in order to reduce the fuel consumption while the local energy demand (both electrical and thermal) and certain minimum reserve power are satisfied. Tsikalakis and Hatziargyriou optimized the operation of the MGs during inter-connected operation by optimizing the generation of the DG units and power exchange with the upstream network [10]. Chedid and Raiman used a linear programming to minimize the average production cost of electric power in a hybrid solar–wind MG while environmental factors were considered [11].

The main flaw associated with previous studies for EOM of the MGs is neglecting the uncertainty in generation patterns, load demand and market prices. The deterministic approaches are dependent on the accuracy of the input data while there are always errors in input data prediction for EOM of MGs. In an open access power market, the market prices and load demand are more unpredictable than before [12,13]. Moreover, because of the random behavior of the wind speed and solar radiation, the solar and wind units generate uncontrollable and fluctuated power [14,15]. Therefore, the validity of the traditional optimization methods should be re-examined under new circumstance [16]. In this regard, new approaches need to be employed to consider the intermittency in input random data and minimize the risk associated with the design and the EOM of MGs under uncertainty [17,18].

The probabilistic methods can be classified in three categories: the Monte Carlo Simulation (MCS) [19], the analytical techniques and the approximate methods. The MCS methods are the most straightforward and accurate one but have the shortcoming of remarkable computational efforts [18]. Analytical techniques need fewer number of simulations but still require complicated mathematical computations [20]. Approximate methods provide a balance between computational efficiency and accuracy [21]. The $2m$ point estimate method (PEM), as an approximate method, is an efficient and reliable method to model the uncertainty in power systems [20]. Although $2m$ PEM employs the deterministic routines to find the statistical moments of the output random variables, it requires much fewer simulations in comparison to MCS methods.

This paper implements the $2m$ PEM to model the uncertainty in hourly load demand, market prices and available output power of solar and wind DG units. The normal and Weibull probability density function (PDF) are used to model the variations of input random variables (IRVs). Moreover, the Gram–Charlier expansion is employed to provide more accurate probability distribution for output random variables. Finally, a self-adaptive gravitational search algorithm (SGSA) is devised to optimize the EOM of the MGs.

The gravitational search algorithm (GSA) is inspired by the law of gravity and mass interactions. The GSA follows the central force optimization (CFO) algorithm [22] but it unlike the CFO uses inverse distance (between two particles) linearly instead of inverse "distance" squared (like gravity) [23]. In GSA method, the individuals are collection of masses which interact with each other using a policy inspired by the Newtonian gravity law and also the laws of motion [23]. In this study, a self-adaptive mutation technique is proposed to enhance the convergence characteristics of the original GSA and make it robust for different problems including various fitness landscapes. In the proposed mutation technique, two moving strategies are offered to avoid premature convergence and being trapped into local optima. Each mass selects one of the

proposed moving patterns proportional to the problem in hand and the current stage of the optimization procedure. The selection technique is carried out using a probabilistic model. In the probability model, the strategy with better performance in previous iterations gets a larger chance of being selected by the individuals. The effectiveness of the proposed technique is verified on a typical MG participates in the open market considering the fuel cell, electrical storage, MT, PV and wind turbine (WT) units.

2. Energy and operation management of a microgrid

2.1. Objective function

The total energy and operating cost of the MG includes the fuel costs of units as well as their start-up/shut-down costs. The objective function can be formulated as follows [3]:

$$\begin{aligned} Min\tilde{f}(\mathbf{X}) &= \sum_{t=1}^{NT} Cost^t \\ &= \sum_{t=1}^{NT}\Bigg\{\sum_{i=1}^{N_g}\Big[u_i^t p_{Gi}^t B_{Gi}^t + Start_{Gi}\times\max\left(0,u_i^t-u_i^{t-1}\right) \\ &\quad + Shut_{Gi}\times\max\left(0,u_i^{t-1}-u_i^t\right)\Big] + \sum_{j=1}^{N_s}\Big[u_j^t p_{sj}^t B_{sj}^t \\ &\quad + Start_{sj}\times\max\left(0,u_j^t-u_j^{t-1}\right) + Shut_{sj} \\ &\quad \times\max\left(0,u_j^{t-1}-u_j^t\right)\Big] + p_{Grid}^t B_{Grid}^t\Bigg\} \end{aligned} \tag{1}$$

where $\mathbf{X} = [X^1\ X^2\ \ldots\ X^t\ \ldots\ X^{NT}]$ and X^t is state variables vector including active powers of units and their related states that can be described as follows:

$$X^t = \left[p_{G1}^t, p_{G2}^t, \ldots, p_{GNg}^t, p_{s1}^t, p_{s2}^t, \ldots, p_{sNs}^t, u_1^t, u_2^t, \ldots, u_{Ns+Ng}^t\right] \tag{2}$$

2.2. Constraints

- Power balance:

$$\sum_{i=1}^{N_g} p_{Gi}^t + \sum_{j=1}^{Ns} p_{sj}^t + p_{Grid}^t = \sum_{D=1}^{N_D} P_{L_D}^t \tag{3}$$

- Real power generation capacity:

$$\begin{aligned} p_{Gi,\min}^t \le p_{Gi}^t \le p_{Gi,\max}^t \\ p_{sj,\min}^t \le p_{sj}^t \le p_{sj,\max}^t \\ p_{grid,\min}^t \le p_{Grid}^t \le p_{grid,\max}^t \end{aligned} \tag{4}$$

- Spinning reserve:

$$\sum_{i=1}^{N_g} u_i^t p_{Gi,\max}^t + \sum_{j=1}^{Ns} u_j^t p_{sj,\max}^t + p_{grid,\max}^t \ge \sum_{D=1}^{N_D} P_{L_D}^t + Res^t \tag{5}$$

- Energy storage limits:

Since there are some restrictions on charge and discharge rate of storage devices during each time interval, the following equation and constraint can be considered:

$$W_{ess}^t = W_{ess}^{t-1} + \eta_{charge} P_{charge}\Delta t - \frac{1}{\eta_{discharge}} P_{discharge}\Delta t \tag{6}$$

$$\begin{cases} W_{ess,\min} \le W_{ess}^t \le W_{ess,\max} \\ P_{charge,t} \le P_{charge,\max};\ \ P_{discharge,t} \le P_{discharge,\max} \end{cases} \tag{7}$$

3. 2*m* point estimate method

In 1975, Rosenblueth proposed the 2*m* PEM for solving probabilistic problems [24]. The Rosenblueth's method was inefficient due to the huge number of simulations required. In 1989, Harr developed a new PEM to overcome the drawback of Rosenblueth's method [25]. Although the Harr's method was computationally more efficient than the prior ones, it was restricted to symmetric variables. Finally, Hong introduced effective point estimate methods suitable for both symmetric and asymmetric variables [26,27]. This paper employs the Hang's 2*m* PEM to model the uncertainty in load demand, the market prices and the available output power of the WT and PV units.

Mathematically, the deterministic EOM of the MGs can be expressed as:

$$S = f(v) \tag{8}$$

where v is the set of input variables, S is the output of EOM problem and f is the set of the energy and operation cost equations.

In order to solve the deterministic EOM problem, all IRVs are considered equal to their forecasted values. However, the real values for some variables may differ from their forecasted values [13] such as the errors in the forecasted available output powers of the WT and PV units. The function f transfers the uncertainty from the IRVs to the output variable. Considering m IRVs, (8) can be written as:

$$S = f(c, z_1, z_2, \ldots, z_m) \tag{9}$$

where c is the set of certain variables, z_l ($l = 1,\ldots,m$) are input variables under uncertainty with the probability function Df_{z_l}.

The idea behind the PEM is to calculate the statistical information of the output variables using the solution set of the deterministic EOM problem for only few estimated values of IRVs. In order to find the statistical moments of the output random variable, 2*m* PEM needs only first few central moments of the IRVs, i.e. the mean μ_{pl}, variance σ_{pl} and skewness $\lambda_{pl,3}$ coefficients. This attribute is a remarkable advantage of the point estimate methods where implementing the features of IRVs is a difficult task to reach [21].

The 2*m* PEM produces two probability concentrations for each IRV, z_l, as $(z_{l,1},w_{l,1})$ and $(z_{l,2},\omega_{l,2})$. The $z_{l,po}$ ($po = 1,2$) is called the poth location of z_l and $\omega_{l,po}$ ($po = 1,2$) is a weighting factor which specifies the importance of the corresponding location in evaluating the statistical moments of the output random variable. The deterministic EOM is simulated 2*m* times in the proposed probabilistic method. In each simulation, one of the IRV is fixed to one of its locations, and the other IRVs are equal to their mean value as follows:

$$\begin{aligned} S_{(l,po)} &= f\left(c, \mu_{z_1}, \mu_{z_2}, \ldots, z_{l,po}, \ldots, \mu_{z_m}\right), \quad po = 1,2, \\ & l = 1,2,\ldots,m \end{aligned} \tag{10}$$

where $z_{l,1}$ and $z_{l,2}$ are the specified locations of the IRV z_l, and μ_{z_l} is the mean value of the left over IRVs. Once the solutions of $2m$ deterministic EOM, $S_{(l,po)}$, are explored, the mean and the standard deviation of the output random variable can be estimated.

The step by step procedure of $2m$ PEM to calculate the moments of the output random variable is summarized as:

Step 1: Define m.
Step 2: Set $E(S^h) = 0$, $h = 1, 2$.
Step 3: Select an uncertain parameter z_l.
Step 4: Calculate the skewness $(\lambda_{z_l,3})$ of the z_l according to the following equation.

$$\lambda_{z_l,3} = \frac{E\left[(z_l - \mu_{z_l})^3\right]}{(\sigma_{z_l})^3} \tag{11}$$

where $E[(z_l - \mu_{z_l})^3] = \sum_{j=1}^{N}(z_{l,j} - \mu_{z_l})^3 \times \mathrm{Prob}(z_{l,j})$, N is the number of observations of z_l and $\mathrm{Prob}(z_{l,j})$ is the probability of each observation $z_{l,j}$ which is determined by the system operator [20].

Step 5: Calculate two standard locations:

$$\xi_{l,po} = \frac{\lambda_{z_l,3}}{2} + (-1)^{3-po}\sqrt{\left(m + \left(\frac{\lambda_{z_l,3}}{2}\right)^2\right)}, \quad po = 1,2 \tag{12}$$

Step 6: Compute two estimated location:

$$z_{l,k} = \mu_{z_l} + \xi_{z_l,k}\cdot\sigma_{z_l}, \quad po = 1,2 \tag{13}$$

Step 7: Calculate the deterministic EOM for the poth estimated location:

$$S_{(l,po)} = f\left(\mu_{z_1}, \mu_{z_2}, \ldots, z_{l,po}, \ldots, \mu_{z_m}\right), \quad po = 1,2, \quad l = 1,2,\ldots,m \tag{14}$$

Step 8: Compute two weighting factors of z_l:

$$\omega_{l,po} = \frac{(-1)^{po}}{m}\frac{\xi_{l,3-po}}{(\xi_{l,1} - \xi_{l,2})}, \quad po = 1,2 \tag{15}$$

Step 9: Update the first and second moment of the output random variable (total energy and operational cost):

$$E\left(S^h\right) = E\left(S^h\right) + \sum_{po=1}^{2}\omega_{l,po}\cdot(S(l,po))^h, \quad h = 1,2 \tag{16}$$

Step 10: Repeat steps 3–9 until all uncertain parameters were taken into account.
Step 11: Compute the mean and standard deviation of the total energy and operational cost.

$$\mu_S = E\left(S^1\right), \quad \sigma_S = \sqrt{E(S^2) - \left(E(S^1)\right)^2} \tag{17}$$

The probability density function of the output random variable can be approximated and plotted using the calculated mean and standard deviation and Gram–Charlier series approach [28].

4. Self-adaptive GSA

4.1. Overview of standard GSA

The GSA is inspired by the Newton's law of gravity [23]. According to the law of gravity, each mass attracts every other one with a 'gravitational force'. The gravitational force between two particles is directly proportional to the product of their masses and inversely proportional to the square of the distance between them. Moreover, based on the Newton's second law, the acceleration of each particle only depends on the overall force acts on it and its mass [29]. In the GSA, each particle is considered as an object, its position is a solution of the problem and its mass is corresponded to its fitness value. The GSA expresses the gravitational force as follows:

$$F_{je}^{k,t} = G^k \times \frac{M_j^k \times M_e^k}{R_{je}^k + \varepsilon} \times \left(X_j^{k,t} - X_e^{k,t}\right) \tag{18}$$

where the gravitational constant decreases during the optimization process as:

$$G^k = G_o \times \exp\left(\varpi \times \frac{Iter}{Iter_{\max}}\right) \tag{19}$$

where G_o and ϖ are two constant set to 100 and 20, respectively [23].

The value of mass of each particle is computed by mapping its fitness value as the following equations:

$$m_j^k = \frac{Fit(\mathbf{X}_j^k) - worst^k}{best^k - worst^k} \tag{20}$$

$$M_j^k = \frac{m_j^k}{\sum_{e=1}^{N_{swrm}} m_e^k} \tag{21}$$

where $worst^k$ and $best^k$ are the maximum and the minimum fitness values at iteration k (in minimization problems).

In order to give stochastic characteristics to the algorithm, the overall gravitational forces, which exerts on the jth particles, is calculated by the randomly weighted sum of the forces applied by the other particles as follows:

$$F_j^{k,t} = \sum_{e=1, e\neq j}^{N_{swrm}} r_e \times F_{je}^{k,t} \tag{22}$$

The acceleration of each particle is defined as follows:

$$a_j^{k,t} = \frac{F_j^{k,t}}{M_j} \tag{23}$$

Finally, the new position and velocity of each particle are updated by the following equations:

$$V_{new,j}^{k,t} = a_j^{k,t} + r \times V_{old,j}^{k,t} \quad (24)$$

$$X_{new,j}^{k,t} = X_{old,j}^{k,t} + V_{new,j}^{k,t} \quad (25)$$

In order to balance the exploration and exploitation capability of the GSA, only a set of the particles with better fitness values, i.e. bigger mass, are selected to apply their force to the others. Hence, (22) can be rewritten as:

$$F_j^{k,t} = \sum_{e \in kbest, e \neq j} r_e \times F_{je}^{k,t} \quad (26)$$

where *kbest* is the set of the particles with best fitness values. The number of the particles in *kbest* is a function of time which starts with N_{swrm} and decreases linearly to 1.

Analyzing the GSA algorithm, the following points can be deduced:

1. In GSA algorithm, it is expected that particles are attracted by the heaviest (i.e. most optimal) one because the heavier masses exert more powerful gravitational force according to (18).
2. According to the Newton's law, the gravitational force between two particles *j* and *e* is inversely proportional to the $(R_{je})^2$ while in (18), R_{je} is used instead of $(R_{je})^2$. It is because several experiments have shown that this displacement provides better solutions [23].
3. Considering (23), the motion of the heavier masses corresponded to the better solutions is more slowly than the lighter ones. Thus, the GSA algorithm searches the space around the optimal solutions more carefully which enhances the exploitation and local search capability of the algorithm efficiently.
4. The gravitational constant adjusts the accuracy of the GSA. It has a big value at the beginning to improve the exploration power of the algorithm and avoid being trapped in local optima. Also, it decreases during the optimization process to search the space with the higher probability of the optimal solutions more accurately.

4.2. Self-adaptive mutation

This paper proposes a self-adaptive mutation technique to improve the convergence characteristics of the GSA. In this mutation technique, two methods are offered to modify the solutions. Each particle according to a probability model chooses one of these methods. The probability model is based on the ability of each method to provide more optimal solutions. Using this mutation technique, the particles self-adaptively distinguish which of the proposed methods deserves to be employed for the problem in hand or for each stage of the optimization procedure.

Method 1: The GSA is a memory-less algorithm; i.e. the particles do not use the proper information found in previous iterations. This mutation technique is devised to employ information of the best solution found by the algorithm up to now, named Gl_{best} as follows:

$$X_{mut,j}^{k,t} = X_{new,j}^{k,t} + r \times \left(Gl_{best}^{k,t} - l \times Mean^{k,t} \right) \quad (27)$$

Method 2: This mutation method is proposed to improve the diversity of the solutions, alleviate the stagnation and avoid being trapped in local optima. For each particle *j*, three particles are selected randomly as $n_1 \neq n_2 \neq n_3 \neq j$, and a trial solution is created as:

$$X_{trail}^{k,t} = X_{new,n_1}^{k,t} + r \times \left(X_{new,n_2}^{k,t} - X_{new,n_3}^{k,t} \right) \quad (28)$$

Using the following scheme, a mutant solution is achieved:

$$x_{mut,j\theta}^{t} = \begin{cases} x_{trial,j\theta}^{k,t} & \text{if}(r_1 \leq r_2) \\ x_{new,j\theta}^{k,t} & \text{else} \end{cases} \quad (29)$$

where $\theta = 1,2,\ldots,n$ and r_1 and r_2 are two random numbers between 0 and 1.

In the SGSA method, the probability of both mutation methods is considered as $prbptrn_\sigma = 0.5$ ($\sigma = 1,2$) and a parameter named accumulator is assigned for each method as $acum_\sigma = 0$ ($\sigma = 1,2$).

In each iteration, the particles are sorted based on their fitness values while $j = 1$ represents the particle with best fitness value and the $j = N_{swrm}$ stands for the particle with the worst fitness value. The better solution gets the larger weight factor as:

$$w_j = \frac{\log(N_{swrm} - j + 1)}{\log(1) + \cdots + \log(N_{swrm})}, \quad j = 1, \ldots, N_{swrm} \quad (30)$$

The accumulator of each moving strategy is updated as:

$$acum_\sigma = acum_\sigma + \frac{w_{jj}}{N_{method_\sigma}}, \quad jj = 1, \ldots, N_{method_\sigma} \quad (31)$$

where N_{method_σ} is the number of the particles select σth mutation method and w_{jj} ($jj = 1,\ldots,N_{method_\sigma}$) are the weight factors corresponding to them. The excitation probability is calculated as:

$$Prbptrn_\sigma = (1 - \alpha) \times prbptrn_\sigma + \alpha \times \frac{acum_\sigma}{Iter_{\max}} \quad (\sigma = 1,2) \quad (32)$$

where α is a learning rate to control the learning speed in the SGSA algorithm. It is assumed to be 0.142 in this study. Finally, the normalized probability values of the mutation methods are computed as follows:

$$prbptrn_\sigma = Prbptrn_\sigma / (Prbptrn_1 + Prbptrn_2) \quad (\sigma = 1,2) \quad (33)$$

At each generation, each particle chooses the σth mutation method by using the roulette wheel mechanism based on their probability values.

5. Solution methodology

The procedure for implementing the EOM optimization algorithm for an MG can be summarized in the following steps:

Step 1: Set $prbptrn_\sigma = 0.5$ ($\sigma = 1,2$), $acum_\sigma = 0$ ($\sigma = 1,2$), $\alpha = 0.142$.
Step 2: Randomly generate the initial positions of the particles in the feasible range (4).
Step 3: Implement the 2*m* scheme. Calculate the first and the second moments of the total energy and operation cost.
Step 3.1: Constraint handling scheme – the amount of power balance violation is computed for each particle as:

$$PD = \left(\sum_{i=1}^{N_g} p_{Gi}^t + \sum_{j=1}^{Ns} p_{sj}^t + p_{Grid}^t \right) - \sum_{D=1}^{N_D} P_{L_D}^t \quad (34)$$

- If $PD = 0$, go to Step 4.
- If $PD \neq 0$, one of the generated units is selected randomly and PD is subtracted from it. If the allocated capacity of the selected unit violates its constraint, then the position of the particles is fixed to the boundary values. Repeat the Step 3.1.

Step 4: Sort the particles based on their first moment values. Thereafter, determine Gl_{best}, the mean of the population, $worst^k$ and $best^k$.
Step 5: Update the gravitational mass of each particleM_j^k using (20) and (21).
Step 6: Update the overall force which applies on each particle using (22).
Step 7: Calculate the acceleration and the velocity of each particle using (23) and (24).
Step 8: Update the particles position using (25).
Step 9: Implement the 2m scheme as Step 3.
Step 10: For each particle, select one of the mutation methods by the roulette wheel mechanism based on the $prbptrn_\sigma$.
Step 11: Apply the mutation approach. Find the new solution for each particle.
Step 12: Implement the 2m scheme as Step 3.
Step 13: Update the accumulator of both strategies.
Step 14: Update the $prbptrn_\sigma$ ($\sigma = 1,2$).
Step 15: Go to Step 4 until the current iteration number reaches the pre-specified maximum iteration number.

6. Simulation results

In this paper a typical low voltage (LV) MG portrayed in Figs. 1 and 2 is considered as the test system. The MG consists of different DER units such as the MT, a Phosphoric acid fuel cell (PAFC), PV, WT and also NiMH-Battery. The system data is adopted from Ref. [3]. It is supposed that all DG units produce active power at unity power factor, neither requesting nor producing reactive power. Furthermore, there is a power exchange link between the mentioned MG and the utility (LV network) in order to trade energy during a day based on decisions of the microgrid central controller (MGCC).

Table 1 offers the minimum and maximum production limits of the DER units in the mentioned MG. The bid coefficients of the DER units are given in cent of Euro (€ct) per kilo-Watt hour (kWh) as well as the start-up/shut-down cost. As shown Table 1, although the PV and WT units don't use any fuel, their price is much higher than the other units. This fact is because of their high capital cost. The price of these units considers high to assign payback cost for the initial outlay or as maintenance and renewal costs. The hourly forecasted load demand inner the MG, the normalized forecasted output power of WT and PV and the hourly forecasted market price for a typical day are shown in Fig. 3. The total load demand for the day under studied is 1695 kW. It includes a residential area, one industrial feeder serving a small workshop and one feeder with light commercial consumer as demonstrated in Fig. 1.

It is assumed that the MGCC purchases the maximum available power of the WT and PV at each hour of the day. Moreover, in order to make the analysis simpler, it is supposed that all the units work in electricity mode and no heat load demand is needed.

The SGSA is implemented to solve both deterministic and probabilistic EOM of MG under three scenarios. The first scenario (S_1) is considered to compare the results of the proposed method with those of presented in Ref. [3]. In this scenario, it is assumed that all units are in "on" mode during the examined period and also the initial charge of the NiMH-Battery is infinitive. In second scenario (S_2), the NiMH-Battery acts as S_1 but all the units are allowed to start-up or shut-down for flexible operation of the MG.

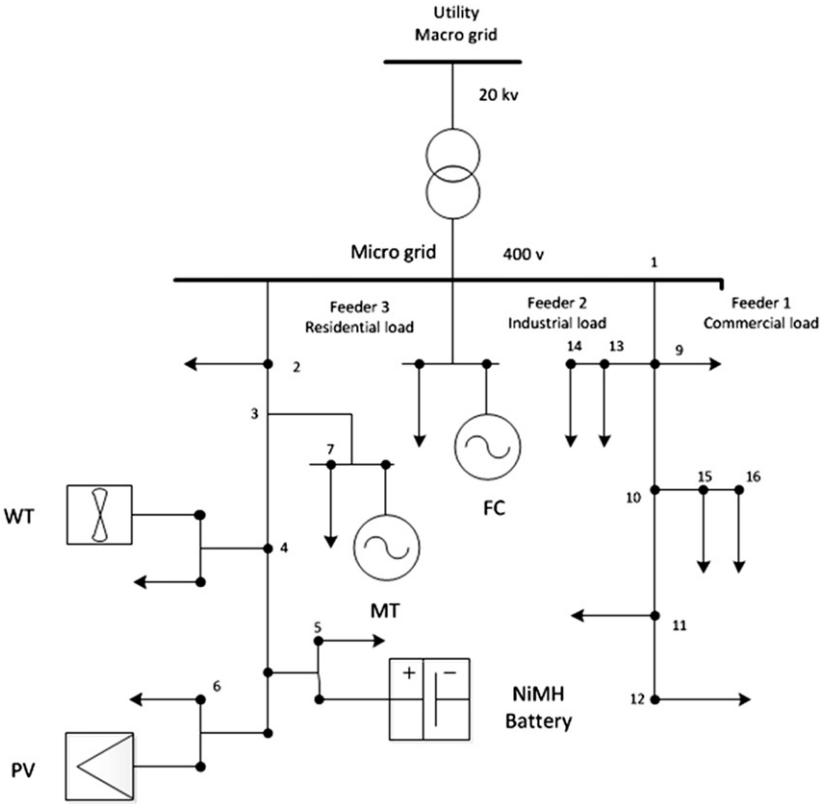

Fig. 1. A typical LV microgrid model.

In the third scenario (S_3), similar to S_2, both "on" or "off" modes can be selected for each unit but the NiMH-Battery starts the examined period with no charge, so in each hour of the day, discharging action of the battery is restricted to how much it is charged in previous hours. The number of the population is considered to be 32 in all simulations.

6.1. Deterministic analysis

In the deterministic EOM of the MGs, it is assumed that the output powers of the WT and the PV units are equal to their forecasted values and the remaining part of the load demand is satisfied by the other DG units. Tables 2–5 give the comparative results of the proposed method versus that of presented in Ref. [3] in terms some statistical indices. Moreover, the results obtained by the original GSA are summarized in the same tables to analyze the effects of the proposed self-adaptive mutation technique on the performance of the SGSA. The results are extracted from 50 independent runs. Tables 2–4 confirm that the proposed SGSA provides higher quality solutions and faster convergence characteristics in comparison with the other cited methods. For S_1, the SGSA converges to optimum solution after 960 objective function evaluations (OFEs). The required OFE for the other methods are not only several times more than those of the SGSA, but also they are trapped in local optima after huge number of OFEs. At each iteration, the number of OFEs using the GSA and SGSA are equal to N_{swrm} and $2 \times N_{swrm}$, respectively. Although at each iteration, the number of OFEs using the SGSA is more than GSA, the SGSA converges to optimum solutions after fewer number of iterations and its final number of OFEs is much fewer than the GSA. Considering Tables 2–4, it is obvious that employing self-adaptive mutation technique not only accelerates the convergence of the GSA, but also enables it to alleviate the stagnation and escape from local optima. It means that the proposed SGSA can provide higher quality and more robust solutions. The calculated standard deviation (STD) of SGSA for S_1 and S_2 is equal to zero which confirms the excellent robustness of the SGSA. In case of the third scenario (S_3), the STD of SGSA has a negligible value as 0.0018 which also confirms the reliability of the proposed method. It is notable that solving the EOM of the MG in scenario S_3 is more complicated than other scenarios because in this scenario there is more sever restriction on the discharging action of the battery. Tables 2–4 also declare the inadequacy of the GSA and other cited methods in this scenario It can be concluded that for more complicated optimization problems, the effectiveness of the proposed mutation technique is more impressive.

Table 1
The limits and bids of the installed DG sources.

ID	Type	Min power (kW)	Max power (kW)	Bid (€ct/kWh)	Start-up/shut-down cost (€ct)
1	MT	6	30	0.457	0.96
2	PAFC	3	30	0.294	1.65
3	PV	0	25	2.584	0
4	WT	0	15	1.073	0
5	Bat	−30	30	0.38	0
6	Utility	−30	30	–	–

Tables 6–8 demonstrate the detail data for the best solution using the SGSA in scenarios S_1, S_2 andS_3, respectively. By analyzing these tables, it can be deduced that all equality and inequality constraints are satisfied. In S_1, all units are in "on" mode, so the MGCC has to purchase at least minimum allowed power of all units even if this policy is not economical. The total energy and operational cost for this scenario is more than the second one which can be studied in Tables 2 and 3. In scenario S_1, the MT units are limited to their minimum values during most hours of the examined period because they generate expensive electrical power. For the same reason, in scenario S_2, the MT units are off during several hours of the day. Besides, during 18–20 pm, the MT is in "on" mode and fixed to its minimum value to satisfy the spinning reserve constraint. The required spinning reserve for hour t is considered $1.05 \times P_{L_p}^t$. The MGCC has to buy electric power from the MT units in scenario S_3 more than scenario S_2. This is because the discharging action of the battery is restricted in scenario S_3. In all scenarios,

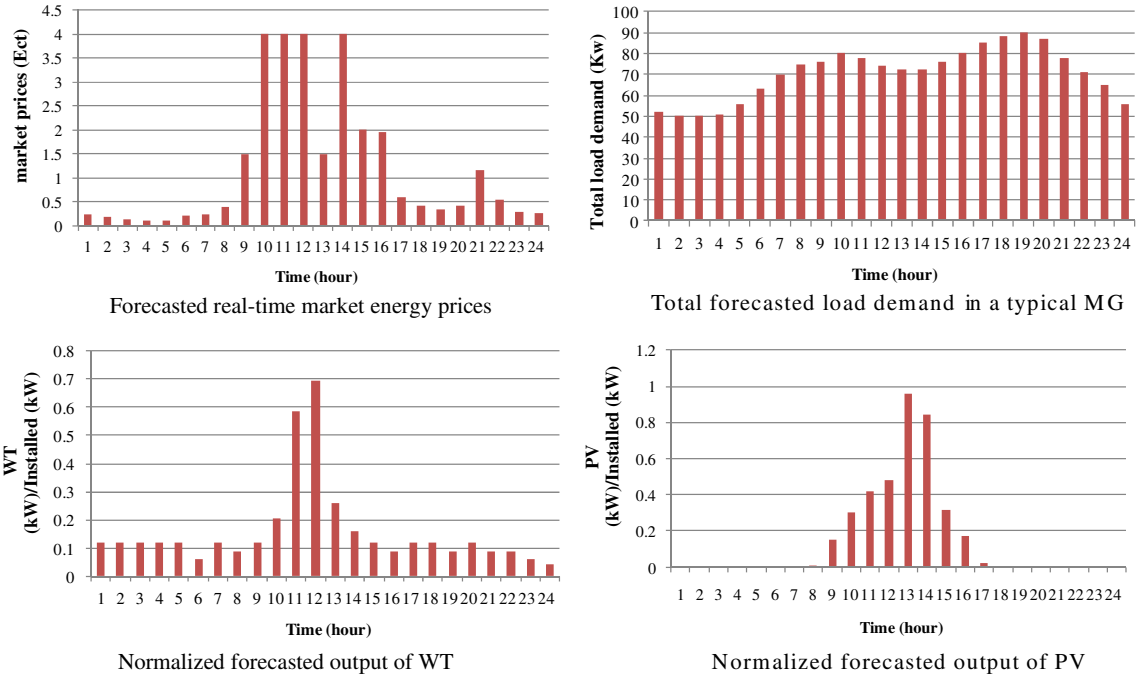

Fig. 2. Forecasted values for market energy prices, load demand, output power of WT and PV.

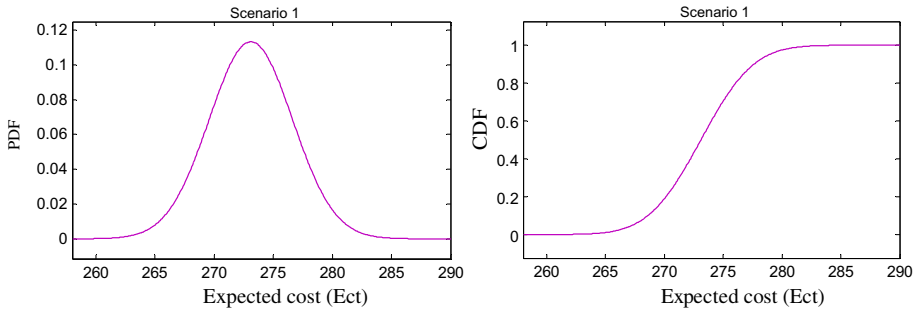

Fig. 3. PDF and CDF of expected cost for scenario 1.

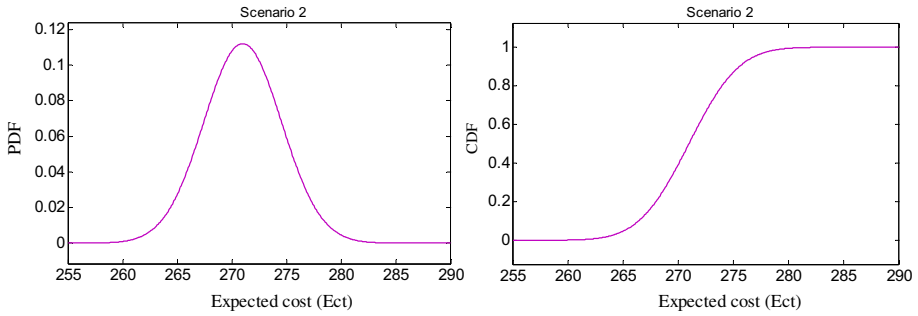

Fig. 4. PDF and CDF of expected cost for scenario 2.

a large portion of load is supplied by the PAFC units within the grid because the bids of these units are lower in comparison to the others.

Since the market price varies hourly, the battery strategy is to store low-price energy during the light-load periods and then release it during the peak hours. During the first hours of the day, the market prices are low. Hence, the MGCC buys active power from the upstream utility through the point of common coupling as much as possible and the surplus energy of the local demand is stored in the batteries. The stored power could be sold to the upstream utility during the peak-load periods. This policy could provide much profit for the MG.

For both scenarios S_1 and S_2, the initial charge of the battery is assumed to be infinitive. Considering the low cost power provided by the battery, it is more economical to buy from it during most hours of the day. In scenario S_3, the battery starts the examined period with no charge. The MGCC buys from the upstream network during first hours of the day, satisfies the local loads and stores the excess power in battery. As the peak-load period starts at 9 am, the battery begins to discharge in order to satisfy the loads and also sells the surplus power of the local loads to the upstream network at high price. During low-price period at 17–20 pm, the algorithm decides to buy from the upstream network and store power in the battery. The battery discharges in 21 pm completely.

Table 2
Comparison of total cost and simulation time for first scenario out of 50 trials.

Method	Best solution (€ct)	Worst solution (€ct)	Average (€ct)	Standard deviation (€ct)	Mean number OFEs	Mean simulation time (min)
GA [3]	277.7444	304.5889	290.4321	13.4421	Up to16,000	–
PSO [3]	277.3237	303.3791	288.8761	10.1821	Up to16,000	–
FSAPSO [3]	276.7867	291.7562	280.6844	8.3301	Up to16,000	–
CPSO-T [3]	275.0455	286.5409	277.4045	6.2341	Up to16,000	–
CPSO-L [3]	274.7438	281.1187	276.3327	5.9697	Up to16,000	–
AMPSO-L [3]	274.5507	275.0905	274.9821	0.3210	Up to16,000	–
AMPSO-T [3]	274.4317	274.7318	274.5643	0.0921	Up to16,000	–
GSA	275.5369	282.1743	277.8021	2.9283	1920	0.013
SGSA	269.7600	269.7600	269.7600	0	896	0.006

Table 3
Comparison of total cost and simulation time for second scenario out of 50 trials.

Method	Best solution (€ct)	Worst solution (€ct)	Average (€ct)	Standard deviation (€ct)	Mean number OFEs	Mean simulation time (min)
GA [3]	277.7444	304.5889	290.4321	13.4421	Up to16,000	–
PSO [3]	277.3237	303.3791	288.8761	10.1821	Up to16,000	–
FSAPSO [3]	276.7867	291.7562	280.6844	8.3301	Up to16,000	–
GSA	274.3740	282.0733	277.6021	2.7294	1920	0.013
SGSA	267.0600	267.0600	267.0600	0	896	0.006

Table 4
Comparison of total cost and simulation time for third scenario out of 50 trials.

Method	Best solution (€ct)	Worst solution (€ct)	Average (€ct)	Standard deviation (€ct)	Mean number OFEs	Mean simulation time (min)
GA	334.3679	345.3569	336.3074	17.7439	Up to 30,000	0.6
PSO	327.9226	340.2094	331.0284	13.7190	Up to 30,000	0.6
FSAPSO	326.7593	335.7240	331.2980	10.3095	Up to 30,000	0.6
GSA	319.6284	331.8401	323.1782	5.0257	9568	0.066
SGSA	304.1147	304.1873	304.1492	0.0108	3840	0.026

6.2. Probabilistic analysis

In the deterministic analysis, it is assumed that the real values of the market prices, load demand and available output powers of the PV and the WT units are equal to their forecasted values. Basically, wind and solar power have stochastic nature. Moreover, in the open access market, there are always errors in forecasted values for market prices. Likewise, the load demands are more unpredictable than before. As a result, the solutions of the deterministic optimization algorithms discussed in the previous subsection are not reliable in the new circumstance.

In this section, the 2m PEM is implemented along with the SGSA to find the optimal distribution of the total energy and operation cost of the MGs. It is assumed that the load demand, market price and the output powers of the PV units have normal distribution. Besides, the Weibull distribution is considered for the output power of the WT units.

Table 8 gives the comparative results of the SGSA against GSA in terms of some statistical indices for all scenarios. As Table 8 shows, the proposed self-adaptive technique improves the convergence

Table 5
Best solutions obtained deterministic EOM problem using SGSA (first scenario).

Time (h)	DG sources (kWh)					
	MT	PAFC	PV	WT	Battery	Utility
1	6	30	0	1.7850	−15.7850	30
2	6	30	0	1.7850	−17.7850	30
3	6	30	0	1.7850	−17.7850	30
4	6	30	0	1.7850	−16.7850	30
5	6	30	0	1.7850	−11.7850	30
6	6	30	0	0.9150	−3.9150	30
7	6	30	0	1.7850	2.2150	30
8	6	30	0.2000	1.3050	20.8499	16.6451
9	30	30	3.7500	1.7850	30	−19.5350
10	30	30	7.5250	3.0900	30	−20.6150
11	28.7750	30	10.4500	8.7750	30	−30
12	21.6400	30	11.9500	10.4100	30	−30
13	14.1850	30	23.9000	3.9150	30	−30
14	18.5800	30	21.0500	2.3700	30	−30
15	30	30	7.8750	1.7850	30	−23.6600
16	30	30	4.2250	1.3050	30	−15.5300
17	30	30	0.5500	1.7850	30	−7.3350
18	6	30	0	1.7850	30	20.2150
19	6	30	0	1.3020	22.6980	30
20	6	30	0	1.7850	30	19.2150
21	30	30	0	1.3005	30	−13.3005
22	30	30	0	1.3005	30	−20.3005
23	6	30	0	0.9150	−1.9150	30
24	6	30	0	0.6150	−10.6150	30

Table 6
Best solutions obtained deterministic EOM problem using SGSA (second scenario).

Time (h)	DG sources (KWh)					
	MT	PAFC	PV	WT	Battery	Utility
1	0	30	0	1.7850	−9.7850	30
2	0	30	0	1.7850	−11.7850	30
3	0	30	0	1.7850	−11.7850	30
4	0	30	0	1.7850	−10.7850	30
5	0	30	0	1.7850	−5.7850	30
6	0	30	0	0.9150	2.0850	30
7	0	30	0	1.7850	8.2150	30
8	0	30	0.2000	1.3050	13.4950	30
9	30	30	3.7500	1.7850	30	−19.5350
10	30	30	7.5250	3.0900	30	−20.6150
11	28.7750	30	10.4500	8.7750	30	−30
12	21.6400	30	11.9500	10.4100	30	−30
13	14.1850	30	23.9000	3.9150	30	−30
14	18.5800	30	21.0500	2.3700	30	−30
15	30	30	7.8750	1.7850	30	−23.6600
16	30	30	4.2250	1.3050	30	−15.5300
17	30	30	0.5500	1.7850	30	−7.3350
18	6	30	0	1.7850	30	20.2150
19	6	30	0	1.3020	22.6980	30
20	6	30	0	1.7850	30	19.2150
21	30	30	0	1.3005	30	−13.3005
22	30	30	0	1.3005	30	−20.3005
23	0	30	0	0.9150	4.0850	30
24	0	30	0	0.6150	−4.6150	30

Table 7
Best solutions obtained deterministic EOM problem using SGSA algorithm (third scenario).

Time (h)	DG sources					
	MT	PAFC	PV	WT	Battery	Utility
1	20.5996	30	0	1.7850	−29.9987	29.6141
2	18.8190	29.5361	0	1.7850	−30.0000	29.8600
3	18.1167	30	0	1.7850	−29.9017	30.0000
4	19.5263	29.6274	0	1.7850	−29.8860	29.9472
5	24.5750	29.7737	0	1.7850	−30.0000	29.8663
6	29.8372	30	0	0.9150	−27.7522	30.0000
7	30	30	0	1.7850	−21.7850	30.0000
8	30	30	0.2000	1.3050	−16.2252	29.7202
9	30	29.9924	3.7500	1.7850	29.9964	−19.5238
10	30	30.0000	7.5250	3.0900	30.0000	−20.6150
11	30	29.9902	10.4500	8.7750	28.7660	−29.9812
12	30	30	11.9500	10.4100	21.5902	−29.9502
13	30	30	23.9000	3.9150	14.1850	−30.0000
14	29.9949	29.9821	21.0500	2.3700	18.5729	−29.9698
15	30	30	7.8750	1.7850	30.0000	−23.6600
16	30	29.9933	4.2250	1.3050	29.9942	−15.5175
17	30	30	0.5500	1.7850	−7.3350	30.0000
18	29.9591	29.9836	0	1.7850	−3.7278	30.0000
19	30	30	0	1.3020	−1.3020	30.0000
20	30	30	0	1.7850	−4.7850	30.0000
21	30	30	0	1.3005	29.5939	−12.8944
22	29.9544	29.9843	0	1.3005	−0.0284	9.7892
23	6.5963	29.9421	0	0.9150	−2.0288	29.5754
24	6.4308	29.8261	0	0.6150	−10.8719	30.0000

Table 8
Affects of the proposed modifications on values of the first moment of probabilistic EOM problem for all scenarios (50 runs).

Type		Best solution (€ct)	Worst solution (€ct)	Average (€ct)	Standard deviation (€ct)	Mean number of OFE	Mean simulation time (min)
S_1	GSA	285.092	297.023	287.602	5.21	921,600	6.21
	SGSA	273.098	273.452	273.231	0. 10	368,640	2.47
S_2	GSA	283.948	293.104	286.394	5.19	915,456	6.12
	SGSA	270.964	271.103	271.005	0.10	356,352	2.38
S_3	GSA	331.395	345.295	335.927	6.02	1,228,800	8.22
	SGSA	312.807	313.006	312.981	0.03	737,280	4.92

Table 9
Best solutions obtained probabilistic EOM problem using SGSA algorithm (first scenario).

Time (h)	DG sources (point 1)						DG sources (point 2)					
	MT	PAFC	PV	WT	Battery	Utility	MT	PAFC	PV	WT	Battery	Utility
1	6	30	0	1.3812	−15.7850	28.1599	7.8290	30	0	2.1862	−15.7850	30
2	6	28.2180	0	1.3815	−17.7850	30	6	30	0	2.1860	−16.0295	30
3	6	29.5072	0	1.3818	−19.0391	30	6	30	0	2.1857	−16.0162	30
4	6	28.1864	0	1.3820	−16.7850	30	6	30	0	2.1855	−14.9845	30
5	6	27.9929	0	1.3817	−11.7850	30	7.9853	30	0	2.1857	−11.7850	30
6	6	27.4907	0	0.7078	−3.9150	30	6.0000	30	0	1.1213	−1.3822	30
7	6.0598	30	0	1.3817	−0.4309	30	8.6782	30	0	2.1858	2.1552	30
8	6	30	0.1019	1.0103	17.8818	16.7435	6	30	0.2980	1.5997	17.8818	22.4909
9	30	30	1.9107	1.3816	30	−20.6165	30	30	5.5902	2.1857	30	−18.5166
10	30	30	3.8530	2.3909	30	−19.7223	29.1197	30	11.1999	3.7842	30	−20.6150
11	28.7750	30	5.3710	6.7915	30	−26.3320	25.0953	30	15.5279	10.7466	30	−30
12	22.6626	30	6.1142	8.0573	28.9774	−25.0176	22.6626	30	17.7848	12.7326	24.0026	−30
13	14.5036	30	17.3238	3.0260	29.6814	−25.6716	14.5036	30	30.4813	4.7942	25.3560	−30
14	18.5800	30	16.7182	1.8274	30	−28.2262	13.8708	30	28.3799	2.9050	30	−30
15	30	30	4.0065	1.3815	30	−22.6954	30	29.0157	11.7468	2.1861	30	−23.6600
16	30	30	2.1547	1.0101	30	−16.6017	30	30	6.2950	1.5998	30	−14.4205
17	30	30	0.2797	1.3813	27.0269	−7.3350	30	30	0.8205	2.1862	30	−4.2908
18	6	26.6120	0	1.3813	30	20.2150	9.4247	30	0	2.1862	30	20.2150
19	6	26.4077	0	1.0078	22.7039	29.9975	6	29.9967	0	1.5959	26.2883	29.9975
20	6	26.6380	0	1.3812	30	19.2150	6	30	0	2.1862	30	22.5641
21	26.9013	30	0	1.0065	30	−13.3005	30	30	0	1.5940	30	−10.2308
22	30	30	0	1.0064	30	−23.0897	30	30	0	1.5940	30	−17.5188
23	6	30	0	0.7079	−4.5058	30	8.6318	30	0	1.1219	−1.9150	30
24	6	27.7242	0	0.4761	−10.6150	30	8.3013	30	0	0.7536	−10.6150	30
Cost	226.0361 (€ct)						373.8558 (€ct)					

characteristics of the SGSA in terms of the both faster convergence and accuracy in comparison to GSA. At each iteration, the number of the OFEs for the GSA and SGSA are equal to $2m \times N_{swrm}$ and$2 \times 2m \times N_{swrm}$, respectively. Similar to, at each iteration, the numbers of the OFEs of the SGSA is twice than those of the GSA, but the SGSA needs much fewer OFEs to converge. For all scenarios, the GSA fails to find satisfactory solution even after more than 600,000 OFEs. In scenario S_3, the GSA is trapped in local optima and no more progress is achieved after 1,228,800 OFEs. Considering the average and the STD provided by the SGSA, it can be concluded that the SGSA could give robust and reliable solutions. The STD of the GSA for all scenarios are several times more than those of the SGSA which shows that the proposed mutation technique successfully modifies the GSA and makes it as a powerful algorithm for both deterministic and probabilistic problems. In the SGSA, particles self-adaptively identify which of the mutation methods is more appropriate to be selected.

Table 9 gives two points for the EOM problem. In the first and second points, it is assumed that all IRVs are equal to their first and the second locations, respectively. As given in Table 9, total energy and operational cost of the first point is lower than the second one because the available output power of the expensive WT and the PV units are lower in this point. As it can be seen in Table 9, due to the low bid of the PAFC units, in most hours of the day, they produce their maximum allowed power. Furthermore, the NiMH-Battery is charged at the first hours of the day while the discharging process is postponed to the midday.

During the high price period at 8 am to 16 pm, the battery is discharged and the surplus energy inside the grid is sold to the market.

Figs. 3–5 portray the PDFs and the cumulative density functions (CDFs) of the best obtained solutions for all scenarios. Referring to Figs. 3–5, the random variables are continuous and they are not very different from normal distributions. Besides, microgrid is small but sufficiently large to allow the use of Gram–Charlier series expansion to accurately approximate the distribution for total energy and operational cost. These figures show that the presented method could find optimal production cost efficiently.

Finally, to verify the impact of the considering uncertainty in the decision making, the value of the stochastic solution (VSS) [30] for both scenarios is calculated. The VSS represents how much the MGCC would be willing to spend in order to know the future realization of the problem and cover the uncertainty in the stochastic processes under consideration. The VSS is calculated by subtracting the expected cost (output of the deterministic EOM

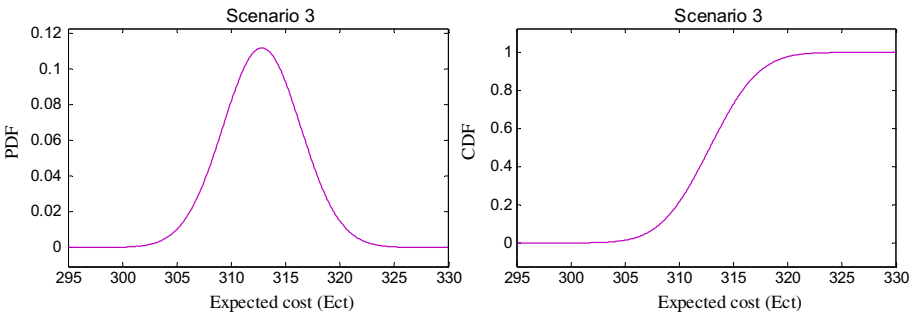

Fig. 5. PDF and CDF of expected cost for scenario 3.

Table 10
Comparison of cases I, II and III of first scenario.

Case	Deterministic	Probabilistic		
	Expected cost (€ct)	Expected cost (€ct)	σ_S	VSS (€ct)
Case I	269.7600	273.000	12.4122	3.24
Case II	445.3263	449.448	13.78	4.12
Case III	668.5674	673.377	14.6	4.81

problem) from the output of the stochastic model. The VSS is 3.2, 3.4 and 8.4 (€ct) for scenarios 1, 2 and 3, respectively.

Table 10 is offered to qualify the relative impact of uncertain sources penetration on the decision making. In this table, the expected cost of both the deterministic and probabilistic models is presented. Table 10 also addressed the σ_S of the total cost distributions and the VSS for scenario S_1 under three cases. In Case I, the maximum installed WT and PV units are as given in Table 1 while in cases II and III WT and PV units are twice and third times larger than what are noted in the Table 10. Referring to Table 10, by increasing the penetration of the uncertain WT and PV units:

1. The expected cost both in deterministic and probabilistic models increase because WT and PV units have higher bids than the other units.
2. The uncertainty in the problem increases accordingly, so the σ_S of the cost distributions (equation (17)) will rise.
3. The VSS increases i.e. the system operator should spend more to know the future realization of the system.

7. Conclusion

This paper proposed a novel probabilistic method for EOM of the MGs under uncertain environment. In the proposed framework, $2m$ PEM was implemented to cover the uncertainties in load demand, market price and the available output powers of the WT and PV units. The Weibull and normal distribution functions were employed to model the IRVs. The SGSA was devised to find the optimal energy planning of the MGs. In the proposed SGSA, a self-adaptive mutation technique was suggested to make it efficient for various problems with different fitness landscapes. This mutation included two powerful moving strategies. The moving methods could effectively overcome the drawback associated with the original GSA. Finally the presented probabilistic method was applied to a typical MG under three scenarios. The PDF and CDF of the total energy and operational cost for all scenarios were achieved using Gram–Charlier expansion. The simulation results showed that the probabilistic approach could provide a more efficient utilization of the uncertain DERs. It also helps the system operators to know how likely uncertainties affect the system and how to handle the related issues. In addition, the results demonstrated that the proposed optimization method could find robust, reliable and high quality solutions in a satisfactory simulation time for energy management problems.

References

[1] Østergaard PA. Reviewing optimisation criteria for energy systems analyses of renewable energy integration. Energy 2009;34(9):1236–45.
[2] Choudhry Mohammad A, Khan Hasham. Power loss reduction in radial distribution system with multiple distributed energy resources through efficient islanding detection. Energy 2010;35(12):4843–61.
[3] Moghaddam A, Seifi A, Niknam T, Pahlavani MR. Multi-objective operation management of a renewable MG (micro-grid) with back-up micro-turbine/fuel cell/battery hybrid power source. Energy 2011;36(11):6490–507.
[4] Obara S, Watanabe S, Rengarajan B. Operation method study based on the energy balance of an independent microgrid using solar-powered water electrolyzer and an electric heat pump. Energy 2011;36(8):5200–13.
[5] Chen C, Duan S, Cai T, Liu B, Hu G. Smart energy management system for optimal microgrid economic operation. IET Renew Power Gener 2011;5(3):258–67.
[6] Dali M, Belhadj J, Roboam X. Hybrid solar–wind system with battery storage operating in grid-connected and standalone mode: control and energy management – experimental investigation. Energy 2010;35(6):2587–95.
[7] Sanseverino E, Silvestre M, Ippolito M, Paola A, Lo Re G. An execution, monitoring and replanning approach for optimal energy management in microgrids. Energy 2011;36(5):3429–36.
[8] Sortomme E, El-Sharkawi MA. Optimal power flow for a system of microgrids with controllable loads and battery storage. IEEE/PES Power Syst Conf; 2009:1–5.
[9] Hernandez-Aramburo C, Green TC, Mugniot N. Fuel consumption minimization of a microgrid. IEEE Trans Ind Appl 2005;41(3):671–81.
[10] Tsikalakis AG, Hatziargyriou ND. Centralized control for optimizing microgrids operation. IEEE Trans Energy Convers 2008;23(1):241–8.
[11] Chedid R, Raiman S. Unit sizing and control of hybrid wind solar power systems. IEEE Trans Energy Convers 1997;12(1):79–85.
[12] Soroudi A, Ehsan M, Caire R, Hadjsaid N. Possibilistic evaluation of distributed generations impacts on distribution networks. Trans Power Syst 2011;4:2293–301.
[13] Soroudi A, Aien M, Ehsan M. A probabilistic modeling of photo voltaic modules and wind power generation impact on distribution networks. IEEE Syst J 2011;99:1–10.
[14] Pantoš M. Stochastic optimal charging of electric-drive vehicles with renewable energy. Energy 2011;36(11):6567–76.
[15] Carta José A, Velázquez Sergio. A new probabilistic method to estimate the long-term wind speed characteristics at a potential wind energy conversion site. Energy 2011;36(5):2671–85.
[16] Hethey J, Leweson S. Probabilistic analysis of reactive power control strategies for wind farms. Master thesis, Technical University of Denmark; 2008.
[17] Anders GJ. Probability concepts in electric power systems. New York: Wiley; 1990.
[18] Morales JM, Perez-Ruiz J. Point estimate schemes to solve the probabilistic power flow. IEEE Trans Power Syst 2007;22:1594–601.
[19] Rubinstein RY. Simulation and the Monte Carlo method. New York: Wiley; 1981.
[20] Su C-L. Probabilistic load-flow computation using point estimate method. IEEE Trans Power Syst 2005;20(4):1843–51.
[21] Malekpour AR, Niknam T. A probabilistic multi-objective daily Volt/Var control at distribution networks including renewable energy sources. Energy 2011;36(5):3477–88.
[22] Rashedi E, Nezamabadi-pour H, Saryazdi S. GSA: a gravitational search algorithm. Inf Sci 2009;179:2232–48.
[23] Formato RA. Central force optimization: a new meta-heuristic with applications in applied electromagnetics. Prog Electromagn Res 2007;77:425–91.
[24] Rosenblueth E. Point estimates for probability moments. Proc Nat Acad Sci USA 1975;72:3812–4.
[25] Harr E. Probabilistic estimates for multivariate analysis. Appl Math Model 1989;13(5):313–8.
[26] Hong HP. An efficient point estimate method for probabilistic analysis. Reliab Eng Syst Saf 1998;59:261–7.
[27] Soroudi A, Ehsan M, Caire R, Hadjsaid N. Hybrid immune-genetic algorithm method for benefit maximisation of distribution network operators and distributed generation owners in a deregulated environment. IET Gener Transm Dist 2011;4:961–72.
[28] Zhang P, Lee ST. Probabilistic load flow computation using the method of combined cumulants and Gram–Charlier expansion. IEEE Trans Power Syst 2004;19:676–82.
[29] Holliday D, Resnick R, Walker J. Fundamentals of physics. John Wiley and Sons; 1993.
[30] Morales JM. Impact on system economics and security of a high penetration of wind power. Ph.D. dissertation, Dept. Electr. Eng., Univ. Castilla-La Mancha, Ciudad Real, Spain; 2010.